International Journal of Science and Research (IJSR)
ISSN (Online): 2319-7064
Impact Factor (2012): 3.358

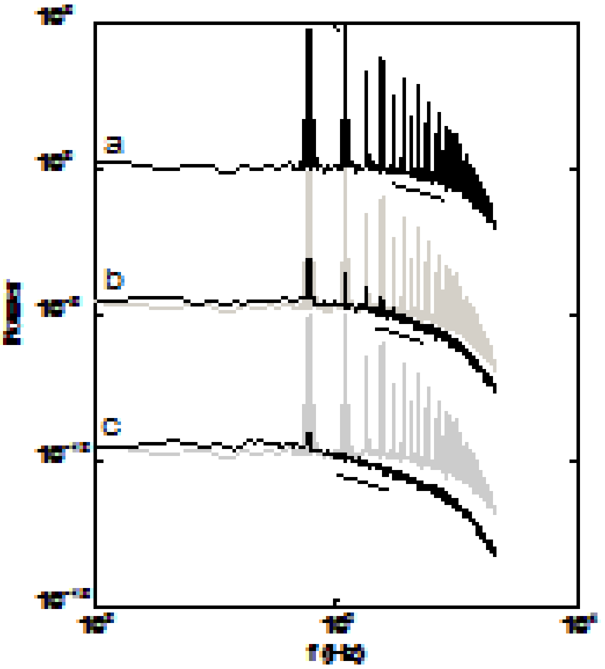

Figure 4: Power spectrum of the centerline velocity ((a): y/e=3, (b): y/e=59, (c): y/e=83).

Forcing frequency f = 60 Hz, forcing amplitude =20 Vc-c.

3.1.2 PIV measurement: Phase-Average Velocity Field

The velocity fields obtained at four significant instants, or phases, of the injection cycle: 0° at the end of the suction, 90° when the membrane is moving up with the maximum velocity, 180° at the end of the ejection and 300° when the membrane is moving down with the minimum velocity are plotted in figure 5. The phase 0°, which corresponds to the end of suction, is given in the first vector fields of Fig.5a. The fluid is expelled out of the cavity through the slot as the membrane moves upwards. The ejection and suction alternation promotes the displacement of the vortices formed by the previous ejection far from the slot. These vortices roll up to form a pair of contra-rotary vortex (Fig.5b). As the membrane moves down, it entrains external fluid through the slot (Fig.5c). However, since the vortices have already traveled away from the slot, they are not affected by the motion of the entrained fluid (Fig.5d).

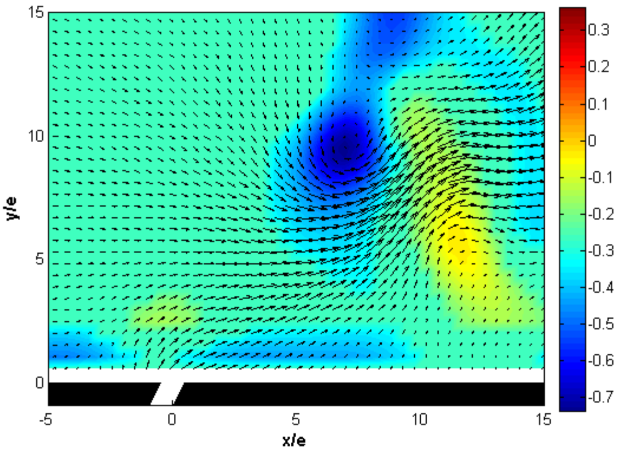

(a)

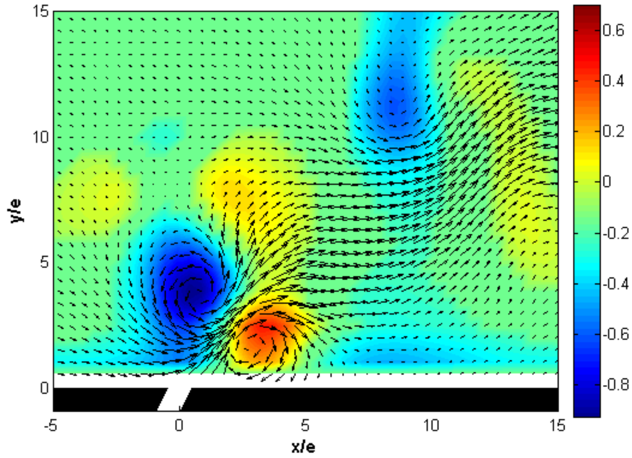

(b)

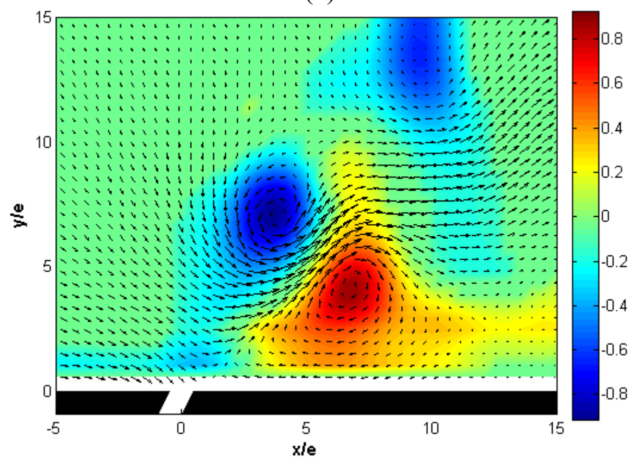

(c)

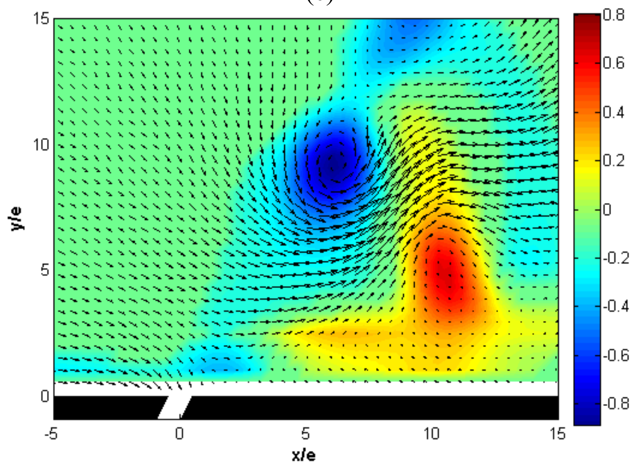

(d)

Figure 5: Phase-average velocity fields. (a) $\phi=0°$, (b) $\phi=90°$, (c) $\phi=180°$, (d) $\phi=300°$

3. 2 Characterization of the flow without control

The mean velocity field is presented in Figures 6 and 7. Without control, the streamlines indicate the formation of a large separation in the region limited by the free flow and the wall. The mean velocity fields indicated that the size of separated zone was influenced by the velocity of the free flow (Fig.6.a, Fig.6.b). In addition, this separated zone is influenced by the inclination of the ramp (Fig.7.a, Fig.7.b).

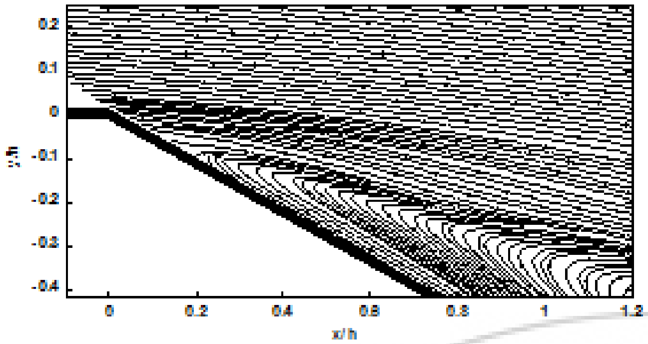

(a)

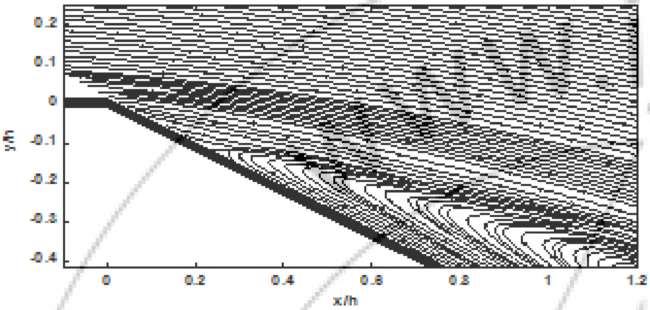

(b)

Figure 6: Streamlines at different cross-flow velocity, β=30°, (a) Without control, U∞=5m/s, (b) Without, control U∞=15m/s

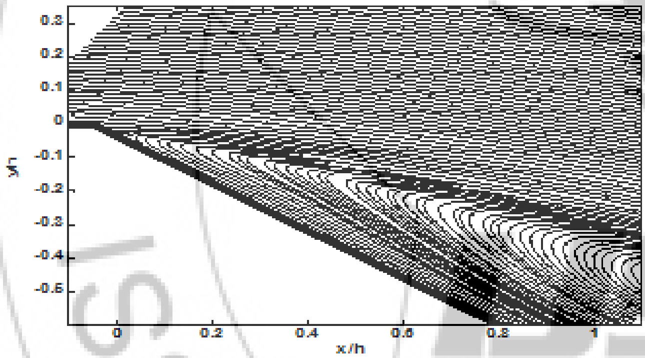

(a)

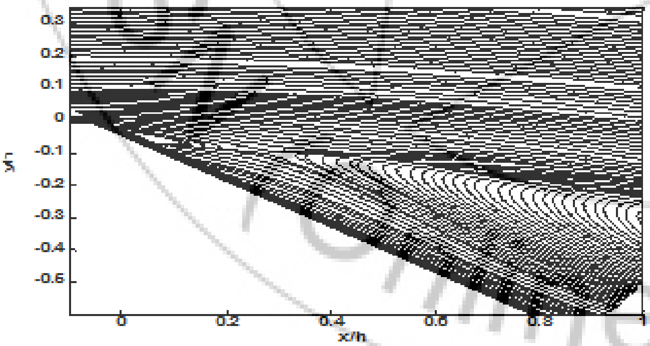

(b)

Figure 7: Streamlines at different cross-flow velocity, β=35°, (a) Without control, U∞=5m/s, (b) Without control, U∞=15m/s

3. 3 Separated flow control with synthetic jet actuator
3.3.1 Mean velocity fields

Fig. 8 and Fig. 9 show the effect of cross-flow velocity. Two different cross-flow velocities have been used: 5 and 15 m/s. The synthetic jet frequency applied is equal to 60 Hz. In this part, the synthetic jet effect on the flow for two inclinations of the ramp (30 ° and 35 °) is studied. Figure 8 shows the actuator effect when the ramp inclination is equal to 30°. In this case the separation is suppressed or delayed. However for the ramp inclination of 35 ° the synthetic jet actuator is unable to eliminate the separation flow (Fig.9). In this last case, the size of the separation is increased. The same control effects have been observed on Ahmed body with inclined rear window at 25° and 35° [12].

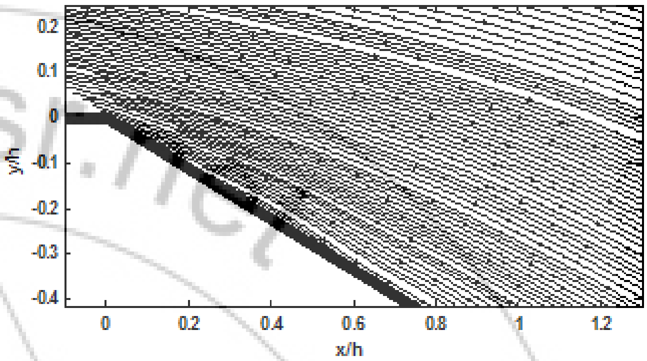

(a)

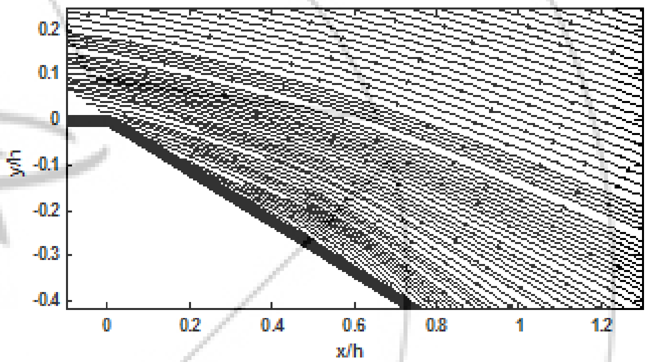

(b)

Figure 8: Streamlines at different jet velocity, β=30°, (a) With control, U∞=5m/s, 60Hz, 10Vcc, (b) With control, U∞=15m/s, 60Hz, 20Vcc

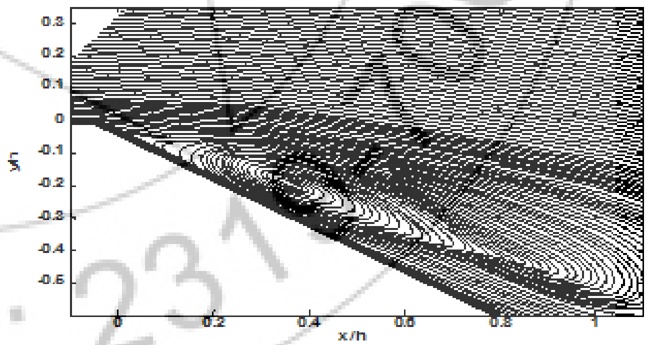

(a)

International Journal of Science and Research (IJSR)
ISSN (Online): 2319-7064
Impact Factor (2012): 3.358

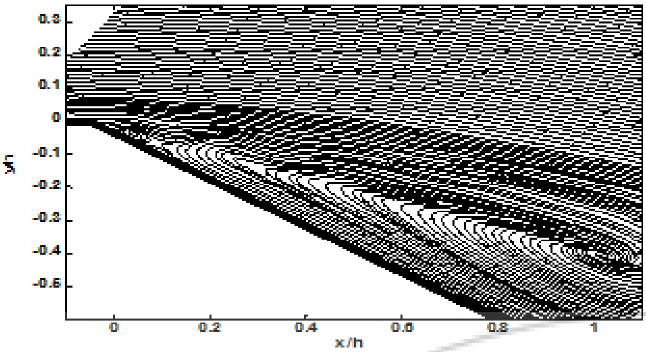

(b)

Figure 9: Streamlines at different jet velocity, β=35°,(a) With control, U∞=5m/s, 60Hz, 15Vcc, (b) With control, U∞=15m/s, 60Hz, 25Vcc

3.3.2 Mean velocity Profiles

The synthetic jet actuator has sufficient velocity u output to produce strong longitudinal vortices. Fig. 10 shows the effect of forcing amplitude at a forcing frequency of 60 Hz. There were four different forcing amplitudes, 10, 15, 20 and 25Vcc, and 60 Hz forcing frequency applied with jet on. The velocity, U was normalized by the local external velocity; u/U was the normalized mean velocity and the boundary layer thickness is denoted by delta.

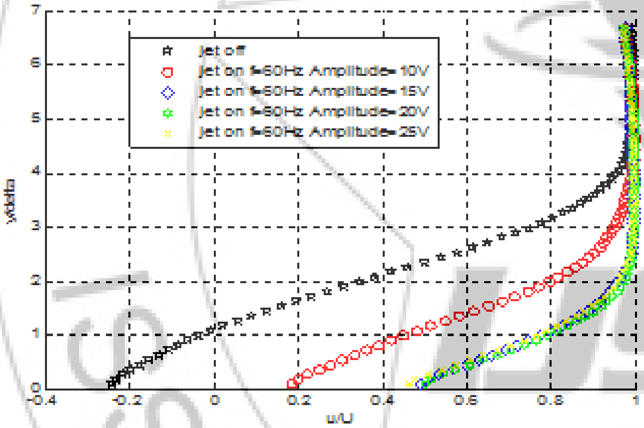

(a)

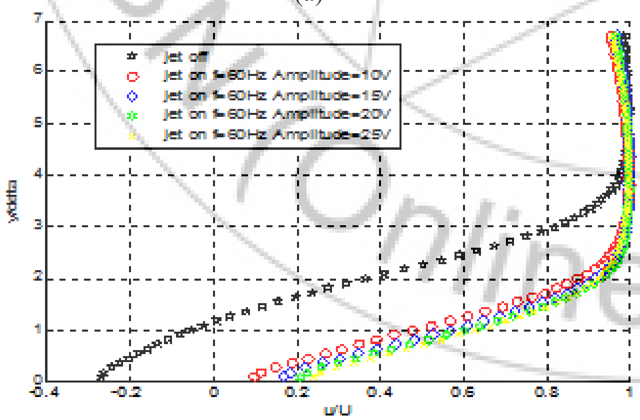

(b)

Figure 10: Velocity in the radial direction for the amplitude forcing frequency 60Hz-angle β=30° - (a) velocity 5m/s (b) velocity 15m/s

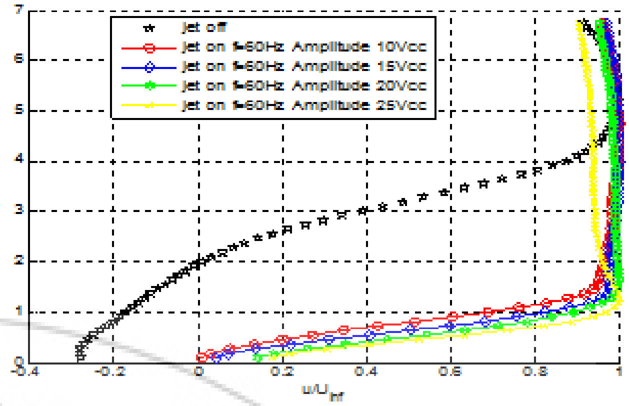

(a)

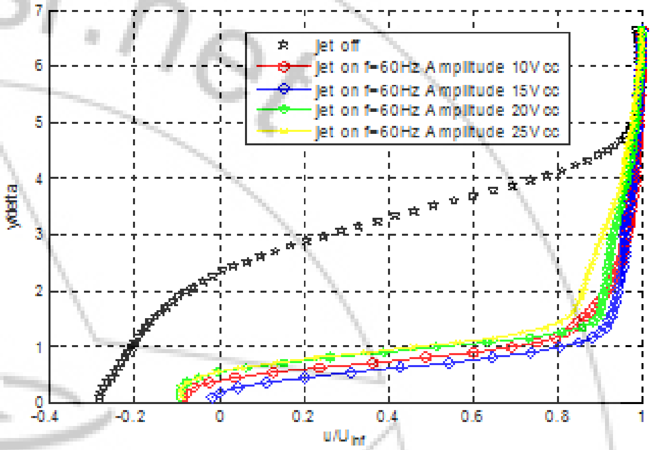

(b)

Figure 11: Velocity in the radial direction for the amplitude forcing frequency 60Hz-angle β= 35° - (a) velocity 5m/s (b) velocity 15m/s

The mean velocity profile was hardly changed when the forcing amplitude was 10Vcc. When forcing amplitude is just over 10Vcc, the effectiveness of the flow control seems to be stable when the cross-flow velocity is upper the 5m/s. Thus, it would appear that a critical forcing amplitude exists, below which the control effect of the present actuator is negligible (Fig.10). In the case where the inclination angle is in the vicinity of 35° or more, the figure 11 shows that the actuator is unable to eliminate the flow separation.

4. Conclusion

Synthetic jet actuator in this work has been introduced and demonstrated the feasibility of active separated boundary layer control in turbulent flows. The interaction of synthetic jet, with either a straight or inclined slot, with a quiescent environment and a cross-flow was documented experimentally. For the case of quiescent environment, we observe a mean flow in spite of the alternative injection. The phase-average velocity fields indicate the generation of a pair of vortices at the beginning of the blowing phase and their advection during the following phase. The control on the boundary layer seems to depend strongly to the forcing voltage. The synthetic jet actuators must have sufficient velocity output to produce strong longitudinal vortices if they are to be effective for flow control. The results obtained have shown that the synthetic jet actuator is an effective and promising device for controlling separation in an adverse pressure gradient boundary layer under the condition that the angle of inclination of the ramp remains below 35 °.

References

[1] P. Gillero, Modèles analytiques pour la condition limite d'un contrôle par jet pulsé, 20ème Congrès Français de Mécanique, Besançon, 29 août au 2 septembre 2011

[2] V.J. Modi, F. Mokhtarian, M. Fernando, T. Yokozimo, Moving surface boundary layer control as applied to 2-d airfoils, AIAA paper, 1989,pp. 89–0296.

[3] I.Wygnanski, Boundary layer flow control by periodic addition of momentum, in: 4th AIAA Shear Flow Control Conference, Silvertree Hotel Snowmass Village, CO, June 29 – July 2, 1997.

[4] D.C. McCormick, Boundary layer separation control with directed synthetic jets, AIAA paper, 2000-0519, January 2000.

[5] F.G. Collins, Boundary layer control on wings using sound and leading edge serrations, AIAA, 1979, pp. 1979–1875.

[6] P.K. Chang, Control of Flow Separation, Hemisphere, Washington, DC, 1976.

[7] M. Gad-el-Hak, Flow Control, Passive, Active and Reactive Management, Cambridge Univ. Press, Cambridge, UK, 2000.

[8] Glezer. A, Amitay. M (2002). Synthetic jets. Annu. Rev. Fluid Mech. 34, 503–29.

[9] J.-C. Béra, M. Sunyach, M. Michard, G. Comte-Bellot, Changing lift and drag by jet oscillations: experiments on a circular cylinder with turbulent separation, Eur. J. Mech. B Fluids 19 (2000) 575–595.

[10] D.R. Williams, H. Mansy, C. Amato, The response and symmetry properties of a cylinder wake subjected to localized surface excitation, J. Fluid Mech. 234 (1992) 71–96.

[11] S. Aubrun, J. Mcnally, F. Alvi, A. Kourta, Separation flow control on a generic ground vehicle using steady microjet arrays, Experiments in Fluids, 55: 1177-1187, 2011, DOI 10.1007/s00348-011-1132-0

[12] E. Bideaux, P. Bobiller, E. Fournier, P. Gilliéron, P. Gilotte, M. EL Hajem, JY Champagne, A. Kourta, Drag reduction by pulsed jets on strongly unstructured wake: towards the square back control, Int. J. Aerodynamics, Vol. 1, Nos. 3/4, pp 282-298, 2011.

[13] C. Sarraf, H.Djeridi, S.Prothina, J.Y.Billarda, Thickness effect of NACA foils on hydrodynamic global parameters, boundary layer states and stall establishment, Journal of Fluids and Structures 26 (2010) 559–578